

Spin state of negative charge-transfer material SrCoO₃

J. Kuneš,¹ V. Křápek,¹ N. Parragh,² G. Sangiovanni,² A. Toschi,³ and A. V. Kozhevnikov⁴

¹*Institute of Physics, Academy of Sciences of the Czech Republic,
Cukrovarnická 10, Praha 6, 162 53, Czech Republic*

²*Institut für Theoretische Physik und Astrophysik,
Universität Würzburg, Am Hubland, D-97074 Würzburg, Germany*

³*Institut für Festkörperphysik, Technische Universität Wien, Vienna, Austria*

⁴*Institute for Theoretical Physics, ETH Zurich, CH-8093 Zurich, Switzerland*
(Dated: October 14, 2018)

We employ the combination of the density functional and the dynamical mean-field theory (LDA+DMFT) to investigate the electronic structure and magnetic properties of SrCoO₃, monocystal of which were prepared recently. Our calculations lead to a ferromagnetic metal in agreement with experiment. We find that, contrary to some suggestions, the local moment in SrCoO₃ does not arise from intermediate spin state, but is a result of coherent superposition of many different atomic states. We discuss how attribution of magnetic response to different atomic states in solids with local moments can be quantified.

PACS numbers: 75.20.Hr, 71.10.Fd, 75.30.Mb

The microscopic origin of the paramagnetic (PM) moment is one of the key questions in materials with strongly correlated electrons. In particular, local moments with magnitudes far from any atomic limit pose a non-trivial problem. The perovskite cobaltites Sr_xLa_{1-x}CoO₃, an example of such system, attracted much attention. The variety of possible valence and spin states of the Co ion and their nearly degenerate energies are behind the strongly temperature (T) and pressure dependent magnetic susceptibility and conductivity in LaCoO₃ [1] as well as the formation of large magnetic polarons and spin glass in Sr_xLa_{1-x}CoO₃ at small doping x . At larger dopings the material becomes a ferromagnetic (FM) metal [2] and remains so up to the stoichiometric SrCoO₃ composition [3]. Fractional PM moment in LaCoO₃ is traditionally thought to arise from the statistical mixture of the low spin (LS) ground state and high spin (HS) or intermediate spin (IS) excited state. While the IS state cannot be the ground state of an isolated ion in a crystal-field, it was suggested that it may be stabilized by the covalent Co-O bonding [4–6]. SrCoO₃ is considered a candidate for realization of IS ground state [6, 7].

Is it possible to associate the PM moment with a particular atomic state or states in materials with strong metal-ligand hybridization? Can we quantify the contributions of different states? We address these questions in the case of SrCoO₃ and propose a general way to answer them. To this end we employ the LDA+DMFT approach [8] to compute the k -resolved spectral functions, the reduced density matrix for the Co site, and local two-particle correlation functions including the local spin susceptibility. SrCoO₃ is found to be metallic both in PM and FM phase. We show that its PM moment cannot be associated with either IS or HS state of Co.

The calculation proceeds in several steps. First, an

LDA calculation for the experimental perovskite structure is performed using WIEN2k [9] density functional code. The converged bandstructure is represented in the Wannier function basis [10] spanning the Co d and O p bands. The averaged screened Coulomb and exchange parameters for the Co- d orbitals $U=10.83$ eV and $J=0.76$ eV were derived using the constrained RPA technique [11]. Following the ideas of Ref. 12, we screen the bare Coulomb interaction by a reduced polarization, which doesn't contain transitions within O p – Co d band complex.

Then we construct a multi-band Hubbard Hamiltonian

$$H = \sum_{\mathbf{k}} \begin{pmatrix} \mathbf{d}_{\mathbf{k}}^{\dagger} \\ \mathbf{p}_{\mathbf{k}} \end{pmatrix} \begin{pmatrix} h_{\mathbf{k}}^{dd} - \epsilon_{\text{dc}} & h_{\mathbf{k}}^{dp} \\ h_{\mathbf{k}}^{pd} & h_{\mathbf{k}}^{pp} \end{pmatrix} \begin{pmatrix} \mathbf{d}_{\mathbf{k}} \\ \mathbf{p}_{\mathbf{k}} \end{pmatrix} + \sum_i W_i^{dd}$$

Here $\mathbf{d}_{\mathbf{k}}$ ($\mathbf{p}_{\mathbf{k}}$) is an operator-valued vector whose elements are Fourier transforms of $d_{i\alpha}$ ($p_{i\gamma}$), which annihilate the Co d (O p) electron in the orbital α (γ) in the i th unit cell. We have used two types of on-site interaction W_i^{dd} : i) the simplified one of the density-density form $w_{\alpha\beta} n_{\alpha} n_{\beta}$ and ii) the SU(2) symmetric interaction of the general form $\tilde{w}_{\alpha\beta\gamma\delta} d_{\alpha}^{\dagger} d_{\beta}^{\dagger} d_{\gamma} d_{\delta}$ in the Slater-Kanamori parametrization [13]. The double-counting term ϵ_{dc} approximately corrects for the explicitly unknown mean-field part of the interaction coming from LDA. At each DMFT iteration ϵ_{dc} is obtained as the the orbital average of the high-frequency self-energy, $\epsilon_{\text{dc}} = \overline{\Sigma(\omega \rightarrow \infty)}$, which equals the orbitally averaged Hartree energy. The effective Weiss field is obtained by iterative solution of the DMFT equations [14] using the finite temperature Matsubara formalism and continuous time quantum Monte-Carlo (QMC) method. The numerical demands of solving the problem with the simplified interaction (i) [15] are substantially smaller than in the SU(2) symmetric case (ii) [16]. Combining the two allows us to investigate a variety of observables without oversimplifying the problem.

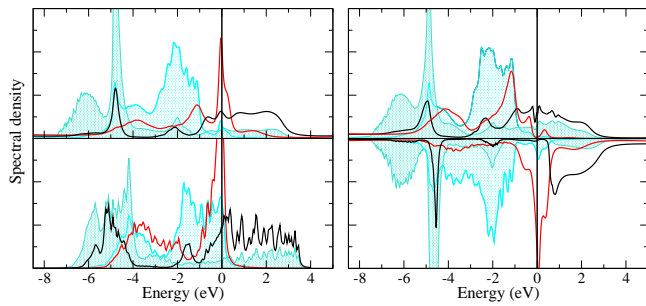


FIG. 1: (color online) The spectral density per orbital: Co $d-e_g$ (black), Co $d-t_{2g}$ (red), O p_σ (darker blue), p_π (lighter blue) in the PM DMFT (upper left), in LDA (lower left) and in FM DMFT (right panel) solution. The minority spin in the FM phase is distinguished by the minus sign.

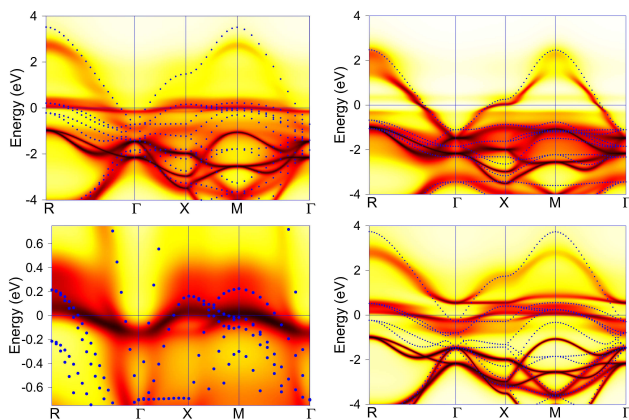


FIG. 2: The k-resolved spectral function $A_{\mathbf{k}}(\omega)$ along the high symmetry directions presented as a color plot of $A_{\mathbf{k}}(\omega)/(2 + A_{\mathbf{k}}(\omega))$. The PM solution is compared to the LDA bands (dots) in the upper left and in detail in the lower left panel. The same spectral function in the FM phase resolved into the majority (upper right) and minority (lower right) spin channels. The LDA bands are marked with dots.

First, we discuss the one-particle dynamics obtained with the density-density interaction at $T=1160$ K. The PM solution is enforced by the $\langle S_z \rangle = 0$ constraint at each DMFT iteration. Lifting this constraint, FM is the stable phase below 1800 K. The desired spectral functions at real frequencies are obtained by analytic continuation from the Matsubara contour. Following Ref. 17 we used the maximum entropy method [18] to continue the self-energy. The Green functions were constructed from the corresponding Dyson equation. This approach provides a straightforward access to the k-resolved spectra of both d and p electrons.

In Fig. 1 we present the k-integrated DMFT spectra in the PM and FM phases along with the LDA spectra for reference. The dynamical correlations lead to reduction of the Co d occupancy from the LDA value of 7.0 to 6.0. Despite the strong $d-d$ interaction ~ 10 eV the system

remains metallic. Nevertheless, substantial band narrowing and new features (including an incoherent background up to ~ 20 eV) appear in the DMFT spectra. The FM phase exhibits a spin-dependent orbital polarization at the Fermi level (E_F) with the e_g states dominating the majority and the t_{2g} states the minority spin channel.

To distinguish the band dispersion and the quasiparticle broadening we have calculated the k-resolved spectral functions, shown in Figs. 2. Comparison of the PM spectra with the non-interacting LDA bands reveals substantial differences near E_F . Absence of sharp quasiparticles there indicates a strong scattering. In the FM spectra both the majority (e_g) and minority (t_{2g}) quasiparticles around E_F are sharper and while the overall band structure matches better its spin-polarized LSDA counterpart substantial differences around E_F remain. The quasiparticle broadening is quantified in Fig. 3a,b showing the imaginary part of the self-energy, which determines the quasiparticle line-width. While both the PM and the FM self-energies exhibit a dip at E_F , $\text{Im}\Sigma(0)$ is substantially larger in the PM phase and the quasiparticle concept loses its meaning there. To assess the impact of the density-density approximation for our conclusions we have performed PM calculation with the SU(2) symmetric interaction. In Fig. 3c,d we compare imaginary frequency self-energies at a temperature of 232 K, where more pronounced differences are expected. While there is an overall agreement between the two sets of self-energies, differences exist in particular at the lowest Matsubara frequencies. The extrapolation of the e_g self-energy to zero frequency points to a stronger scattering by local moment fluctuations in the density-density approximation. This is plausible since Ising spins pose a bigger obstacle for quasi-particle propagation than the Heisenberg ones as was also found in the studies on a two-band Hubbard model [19].

The reciprocal-space quasiparticle picture is commonly used to discuss the properties of metallic systems, while transition metal oxides are more often described in terms of the direct-space atomic states. The strong coupling QMC solver is particularly useful in this respect as it provides a simple way to compute the reduced density matrix operator for the interacting atom (called state statistics in Ref. [22]). This quantity, which tells ‘how much time the atom spends in a particular many-body state’, allows straightforward evaluation of the expectation value of any local operator. In the inset of Fig. 4a we show the statistics of the valence states (d^5 , d^6 , ...) as well as the atomic multiplets with the largest weights. Contrary to the formal Co^{4+} (d^5) valence, the Co atoms spend most of the time in d^6 configuration with almost symmetric fluctuations to d^5 and d^7 , a feature consistent with metallic behavior [23, 25]. Inspecting the weights of different multiplets (Fig. 4a) we find the d^6 HS state ($\uparrow_3^2\downarrow_1^0$ where the subscripts stand for the number of t_{2g} and superscripts for the number of e_g elec-

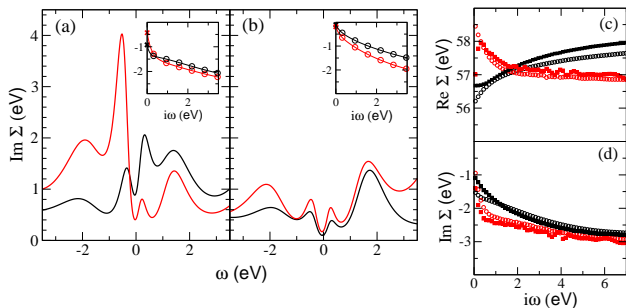


FIG. 3: The imaginary part of the self-energy at $T=1160$ K obtained with density-density interaction in the PM (a) and FM (b) phases. The diagonal Σ_{ee} (black) and Σ_{tt} (red) are shown (for the FM phase only the majority e_g and minority t_{2g}). The insets show the same functions on the imaginary axes together with the values on the Matsubara contour (open symbols). The zero frequency values are highlighted with the crosses. In panels (c) and (d) the real and imaginary parts of the self-energy obtained in the PM phase with the density-density (open circles) and with the SU(2) symmetric (filled squares) interaction at $T=232$ K are compared.

trons) to be most abundant with about 33 %. Since the density-density and SU(2) symmetric interaction leads to different multiplet structures we cannot compare directly the multiplet weights. Nevertheless, we can compare total weights of sectors indexed by charge and the total spin $|S_z|$ (density-density) or $S = \sqrt{S_x^2 + S_y^2 + S_z^2}$ (SU(2)), shown in Fig. 4b, and find a close match. We attribute it to the fact that the dominant HS state is well captured with both forms of the interaction. This does not necessarily mean that all physical quantities are similar. Differences are expected in particular for quantities to which the individual members of the multiplets contribute differently such as the spin susceptibility and thus the FM T_C , which are certainly overestimated with the density-density interaction. [20, 21] To resolve the question of the origin of the local moment we turn our attention to the local spin susceptibility. Large weight of the HS state by itself does not guarantee a Curie-Weiss susceptibility, $\chi \sim 1/T$. It is necessary that the moments are long lived as is clear from the Kubo formula $\chi = \int_0^{\beta=1/T} d\tau \langle S_z(\tau) S_z(0) \rangle$. The spin-spin correlation function along the imaginary time contour obtained with the density-density interaction is shown in Fig. 4. The flattening out after the initial rapid decay is indicative of the local moment behavior. The PM Co moment of $3.06 \mu_B$, estimated by $S_{\text{scr}} = \langle S_z(\beta/2) S_z(0) \rangle$, is close to the saturated FM moment on the Co atom of $2.7 \mu_B$ (which is fairly close to the LSDA value of $2.58 \mu_B$ per u.c. and the experimental saturation magnetization of $2.5 \mu_B$ [3]), shown in the inset. To make contact with the SU(2) symmetric interaction we compare the effective moments derived from the instantaneous correlators $\langle S_z^2 \rangle_{DD} = S_{\text{eff}}^2$ and $\langle S_z^2 \rangle_{SU(2)} = S_{\text{eff}}(S_{\text{eff}} + 1)$. S_{eff} of

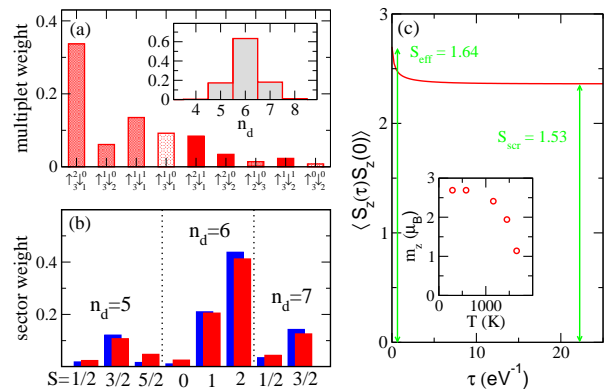


FIG. 4: (a) Weights of the dominant density-density multiplets of the Co d shell at ($T=232$ K). The inset shows the total weights of the different charge sectors (d^5 , d^6 , ...), distinguished by shading in the main panel. (b) Comparison of the weights of different charge and spin sectors obtained with density-density (red) and SU(2) symmetric (blue) interactions. (c) Local spin-spin correlation in the PM phase with the density-density interaction. The inset shows the temperature dependence of the ordered (FM) Co moment.

about 1.64 and 1.61 are obtained in the density-density and SU(2) symmetric calculation, respectively.

The experimental PM moments are often associated with a particular multiplet and a fractional value is interpreted as a mixture of contributions from different multiplets, the thermally induced PM susceptibility in LaCoO₃ being a textbook example. In general, however, it is not possible to divide the susceptibility into multiplet contributions as can be shown by expressing the spin operators S_z in terms of the atomic states projectors P_A

$$\chi = \sum_{A,B} S_z(A) S_z(B) \int_0^{1/T} d\tau \langle P_A(\tau) P_B(0) \rangle,$$

with A and B running over all the atomic many-body states. Contributions of individual multiplets make sense only if the matrix $\Pi_{AB} = \int_0^{\beta} d\tau \langle P_A(\tau) P_B(0) \rangle$ has negligible off-diagonal elements. This means that causal evolution between such states has low probability and their simultaneous population is a result of ensemble averaging. A trivial example is an isolated atom for which Π_{AB} is diagonal in the basis of atomic eigenstates. It is also possible that Π_{AB} has a block structure. In that case each block can be associated with the dominant multiplet and fluctuations around it, arising for example from hybridization with ligands. Examples of such behavior can be found in systems near the high-spin-low-spin transition [22, 24] or systems with fluctuating valence [25].

The state correlation matrix Π_{AB} obtained with density-density interaction (SU(2) symmetric calculation is prohibitively expensive) is presented in Fig. 5 with only the multiplets with large weights shown for simplicity. The depicted part of Π_{AB} contains 70% of the

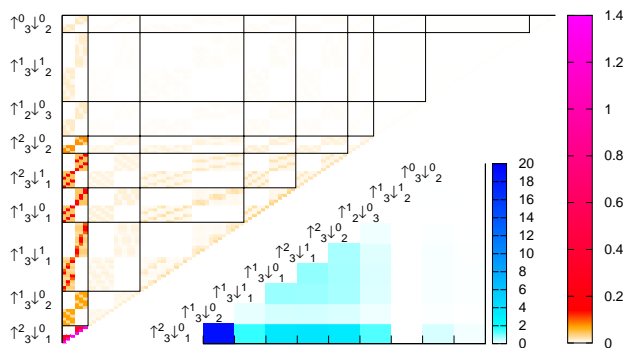


FIG. 5: The atomic state correlation matrix Π_{AB} between the multiplets shown in Fig. 4 obtained with density-density interaction at 232 K. Upper left triangle shows the state-by-state relative contributions. The lower right triangle shows the contribution of multiplet pairs to the local susceptibility.

total $\sum_{A,B} \Pi_{AB} = \beta$. Only states with the same spin orientation exhibit sizable off-diagonal elements, leading to an apparent block structure within each black rectangle. Other than this no block structure can be found which means that all the states are connected by causal evolution. Therefore we cannot view the system as a mixture of HS and IS states and distinguish their contributions to the susceptibility. This statement is quantified in the lower right panel of Fig. 5 where the contributions of the different multiplet pairs to the spin susceptibility are shown. Although the HS-HS contribution is largest it amounts only to 23 % of the total.

There is a connection between the multiplet picture and the one-particle spectra. Even in the PM phase there exists a local spin orientation which is long lived, i.e. there is a strong correlation between the states of this orientation. The local-majority t_{2g} orbitals remain filled, which becomes apparent in the FM spectra. Similarly the minority e_g states are mostly empty except for short visits of the $\uparrow^1\downarrow^1$ configuration, the short life-time of which can be deduced from the relatively small diagonal element of Π_{AB} . These fluctuations are responsible for a saturated Co-O σ -bond and do not lead to metallicity. Based on these observations it is plausible to ascribe the FM order to the double exchange mechanism. Unlike in manganites we cannot describe the systems as local t_{2g} moments plus itinerant e_g electrons. In SrCoO₃ the inter-site exchange is mediated by both the majority e_g and minority t_{2g} electrons. The minority e_g electrons participate in Co-O bonding, but are not active in the double exchange. The calculated transition temperature substantially overestimates the experimental one, while the size of the ordered moment agrees rather well. There are two obvious deficiencies of our theory, the Ising character of the local moments and the lack of inter-site spin-spin correlations. To assess their importance a more complete theory would be necessary.

Previous theoretical studies [6, 7] concluded that IS state dominates the ground state of SrCoO₃. We pass over the fact that these studies used phenomenological parameters while we are using full ‘first-principles’ band-structure and focus on the qualitative aspects. Zhuang *al.* [7] used the unrestricted Hartree-Fock method, which allows the system to settle in a particular atomic state, but does not allow quantum or thermal fluctuations and thus cannot properly describe the competition between electron localization and itinerancy. DMFT does not have these deficiencies and can be considered a systematic improvement over the Hartree-Fock approximation. In the other study, Potze *et al.* [6] used exact diagonalization on a small cluster. They found an IS *cluster* ground state with the dominant (67 %) contribution formed by locking the d^6 atomic HS state on Co, similar to our results, with an anti-ferromagnetically oriented ligand hole. Formation of a bound $d^6\bar{L}$ state with conserved total spin is inevitable in a cluster, because the ligand hole has only one Co partner from which it cannot run away and thus is strongly correlated with its state. The situation in a metallic system may be quite different and the Co-O correlation obtained from the cluster calculation is certainly exaggerated. On the other hand, in DMFT the dynamical Co-O correlation is completely neglected, i.e. the Co atom senses the same average environment with $\sim 1/3$ of a hole per O atom irrespective of its own instantaneous state. In the FM phase some Co-O correlation becomes static, which is reflected in the O p_σ orbitals being polarized opposite to the net magnetization ($-0.03\mu_B$ at 1160 K). The total O polarization is positive due to the p_π orbitals ($0.04\mu_B$ per orbital).

In conclusion, using LDA+DMFT approach we have found that SrCoO₃ is a FM metal with transition temperature in the hundreds K range. In the FM phase the majority (minority) spin states at the Fermi level exhibit a complete e_g (t_{2g}) polarization. Reduced quasi-particle scattering in the FM phase with respect to the PM one points to a negative magneto-resistance effect, but actual transport calculations were not performed. The statistical operator projected on the Co atom is dominated by the d^6 HS state, which is reflected in local fast-probe experiments such as the x-ray absorption [6]. On the other hand, the long-time properties such as the static susceptibility are affected by the causal evolution connecting the different atomic multiplets and thus cannot be inferred from the multiplet weights. Taking into account the proper spin-rotation symmetry of the local interaction alters some quantitative details and clearly confirms the overall picture.

We thank Z. Jiráček, P. Novák and K. Held for numerous discussions. N. P. and G. S. are indebted to M. Ferrero, E. Gull and P. Werner for help and feedback in writing the SU(2)-symmetric code. This work was supported by the Grant No. P204/10/0284 of the Grant Agency of the Czech Republic and by the Deutsche Forschungsgemein-

schaft through FOR 1346 (project ID I597-N16 of the Austrian Science Fund, AT).

-
- [1] K. Asai *et al.*, Phys. Rev. B **40**, 10982 (1989); R. Heikes, R. Mazelsky, and R. Miller, Physica **30**, 1600 (1964); P. Raccah and J. Goodenough, J. Appl. Phys. **39**, 1209 (1968).
- [2] R. Caciuffo *et al.*, Phys. Rev. B **59**, 1068 (1999); M. Itoh *et al.*, J. Phys. Soc. Jpn. **63**, 1486 (1994); M. Señaris Rodriguez and J. Goodenough, J. Solid State Chem. **118**, 323 (1995).
- [3] Y. Long *et al.*, J. Phys.: Condens. Matter **23**, 245601 (2011).
- [4] J. B. Goodenough, Mater. Res. Bull. **6**, 967 (1971).
- [5] M. A. Korotin *et al.*, Phys. Rev. B **54**, 5309 (1996).
- [6] R. H. Potze, G. A. Sawatzky, and M. Abbate, Phys. Rev. B **51**, 11501 (1995).
- [7] M. Zhuang *et al.*, Phys. Rev. B **57**, 13655 (1998).
- [8] K. Held *et al.*, phys. stat. sol. (b) **243**, 2599 (2006); G. Kotliar *et al.*, Rev. Mod. Phys. **78**, 865 (2006).
- [9] P. Blaha *et al.*, *WIEN2K, An Augmented Plane Wave + Local Program for Calculating Crystal Properties*. Technical University Wien, Austria (2001).
- [10] A. A. Mostofi *et al.*, Comput. Phys. Commun. **178**, 685 (2008); J. Kuneš *et al.*, Comput. Phys. Commun. **181**, 1888 (2010).
- [11] F. Aryasetiawan *et al.*, Phys. Rev. B **70**, 195104 (2004); A. Kozhevnikov, A. Eguiluz, and T. Schulthess, SC10 Proceedings of the 2010 ACM/IEEE International Conference for High Performance Computing, Networking, Storage and Analysis, pp. 1-10 (2010).
- [12] T. Miyake *et al.*, J. Phys. Soc. Japan **79**, 044705 (2010).
- [13] A. Georges, L. de' Medici and J. Mravlje, arXiv:1207.3033.
- [14] A. Georges *et al.*, Rev. Mod. Phys. **68**, 13 (1996).
- [15] P. Werner *et al.*, Phys. Rev. Lett. **97**, 076405 (2006); A. Albuquerque *et al.*, J. Magn. Magn. Mater. **310**, 1187 (2007).
- [16] A. M. Läuchli and P. Werner, Phys. Rev. B **80**, 235117 (2009); P. Werner and A. J. Millis, Phys. Rev. B **74**, 155107 (2006); N. Parragh, A. Toschi, K. Held, and G. Sangiovanni, arXiv:1209.0915.
- [17] X. Wang *et al.*, Phys. Rev. B **80**, 045101 (2009).
- [18] J. E. Gubernatis *et al.*, Phys. Rev. B **44**, 6011 (1991).
- [19] A. Liebsch and T. Costi, Eur. Phys. J. B **51**, 523 (2006).
- [20] J. Kuneš *et al.*, Phys. Rev. Lett. **102**, 146402 (2009).
- [21] A. E. Antipov *et al.*, arXiv:1206.3416
- [22] P. Werner and A. J. Millis, Phys. Rev. Lett. **99**, 126405 (2007).
- [23] A. K. McMahan, R. T. Scalettar, and M. Jarrell, Phys. Rev. B **80**, 235105 (2009).
- [24] J. Kuneš and V. Krápek, Phys. Rev. Lett. **106**, 256401 (2011).
- [25] E. R. Ylvisaker *et al.*, Phys. Rev. Lett. **102**, 246401 (2009).